CONDENSED
MATTER
PHYSICS

High-pressure induced magnetic phase transition in half-metallic KBeO$_3$ perovskite

M. Hamlat[1], K. Amara[1], K. Boudia[2], F. Khelfaoui[1],*H. Boutaleb[1]

[1] Laboratory of Physico-chemical studies, Dr Tahar Moulay University of Saida, BP 138 Ennasr, 20000 Saida, Algeria

[2] Laboratory of Physico-chemistry of Advanced Materials, University of Djillali Liabes, 22000 Sidi-Bel-Abbes, Algeria

In this paper, we present the study of the structural, mechanical, magneto-electronic and thermodynamic properties of the perovskite KBeO$_3$. The calculations were performed by the full potential augmented plane wave method, implemented in the WIEN2k code which is based on density functional theory, using generalized gradient approximation. The computed formation energy and elastic constants indicate the synthesizability and mechanical stability of KBeO$_3$. Moreover, our results showed that the latter is a half-metallic material with half-metallic gap of 0.67 eV and an integer magnetic moment of $3\mu_B$ per unit cell. In addition, KBeO$_3$ maintains the half-metallic character under the pressure up to about 97 GPa corresponding to the predicted magnetic-phase transition pressure from ferromagnetic to non-magnetic state. The volume ratio V/V_0, bulk modulus, heat capacity, thermal expansion and the Debye temperature are analyzed using the quasi-harmonic Debye model.

Key words: *perovskite, half-metallic character, mechanical stability, magnetic phase transition, thermodynamic properties*

1. Introduction

The perovskite oxides system ABO$_3$ has attracted much attention because of their properties, according to the choice of elements A and B, including antiferromagnetism (LaTiO$_3$) [1], ferroelectricity (BaTiO$_3$) [2], ferroelasticity (SrTiO$_3$) [3], antiferroelectricity (PbZrO$_3$) [4] , ferromagnetism (YTiO$_3$) [5], half-metal ferromagnets (LiBeO$_3$ [6], KMgO$_3$ [7]). Recently, ferromagnetic materials have been gaining importance in spintronics. Specifically, the focus of the recent research is on the perovskite oxides. Indeed, several recent works were reported such as that of Bouadjemi et al. [8], where they found that the cubic perovskite oxide PrMnO$_3$ presents a half-metallic behavior, Rahman and Sarwar [9] predicted strain- and correlation-induced half-metallic ferromagnetism in BFO (BaFeO$_3$), using DFT calculations. Ali et al. [10] demonstrated that CaFeO$_3$ is half metal. However, with its compression up to a certain critical lattice constant, an abrupt change in the electronic and magnetic properties occurs and the compound loses its integer magnetic moment and becomes metallic. In a recent paper, Khandy et al. [11] showed that BaNpO$_3$ is half-metallic ferromagnet, using modified Becke and Johnson Gradient (spin) Generalized (mBJ-GGA) and Hubbard potential approximations (GGA+U), and it may be utilized for spintronic devices. Few researches were carried out on the half-metallic behavior in perovskite oxides without transition (TM) or rare-earth (RE) elements, such as our previous works on LiBeO$_3$ [6] and KMgO$_3$ [7]. In focusing on finding out more half-metallic perovskites, without d and f elements, we report a theoretical investigation of the structural, elastic, electro-magnetic and thermodynamic properties of the hypothetical compound KBeO$_3$. We compared our results with those available on the Materials

*Corresponding author. E-mail: fraiha_phys@yahoo.fr

Project database [12]. The paper is divided into four sections: after the presented introduction, the second section examines the computational details. The results are reported and discussed in section 3. Finally, the fourth summarizes the results of this work and draws conclusions.

2. Computational methodology

In this study, we calculate the structural, elastic, and magneto-electronic properties of perovskite oxide $KBeO_3$, using the Full Potential Linear Augmented Plane Wave (FP-LAPW), implemented in the code WIEN2k [13] and within the density functional theory (DFT) [14]. Semi-relativistic calculations have been made (the spin-orbit effect is neglected). To treat the potential for exchange and correlations, DFT calculations with (PBE-GGA)[15–17] are used to determine and obtain the magneto-electronic properties of this compound. To control the convergence of the basis set, the plane wave cut-off value of $R_{MT}K_{max} = 8$ is used, and we chose muffin-tin radii (MT) of 2, 1.42, 1.33 a.u. (atomic unit) for K, Be, O respectively. The wave functions inside muffin-tin spheres (MTS) are expanded in terms of spherical harmonics times radial eigenfunctions up to $l_{max} = 10$. In the out of MTS (i.e. interstitial region), the wave functions are expanded in plane waves. For the Fourier charge density expansion of the potential in the interstitial region, G_{max} of 14 $Ry^{1/2}$ is used. The charge convergence of $10^{-5}e$ is applied as a convergence criterion for all calculations performed. The density of states DOS is obtained from the calculated Kohn and Sham eigenvalues on a fine k-grid of $14 \times 14 \times 14$ in the irreducible Brillouin zone, using the tetrahedron method [18].

To investigate the mechanical stability of $KBeO_3$ in its cubic structure, the IRelast software [19], is used to compute the elastic constants. Evidently, for accurate calculations of the elastic properties, a much denser k-point grid is necessary. For that reason, we used a k-point sampling grid of $22 \times 22 \times 22$ in the irreducible Brillouin zone.

3. Results and discussion

This part describes and discuses the structural, mechanical, electronic, magnetic and thermodynamic properties of $KBeO_3$. In addition, we study the pressure effect on its HM stability.

3.1. Equilibrium parameters and mechanical stability

As mentioned above, our considered material is the perovskite oxide $KBeO_3$. Therefore, it is investigated in the cubic structure with the Pm3m (221) space group, where the positions of the atoms are K (0, 0, 0), O (0, 0.5, 0.5) and Be (0.5, 0.5, 0. 5), see figure 1.
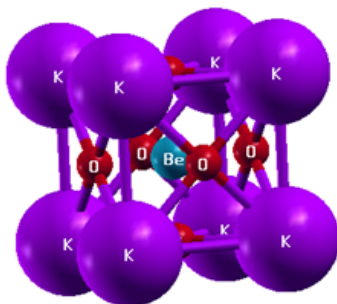

Figure 1. (Color online) Crystal structure of perovskite oxide $KBeO_3$.

In order to determine the magnetic ground state, we calculate the energies for different volumes in the non-magnetic (NM), ferromagnetic (FM), and antiferromagnetic (AFM) phases. The equilibrium lattice
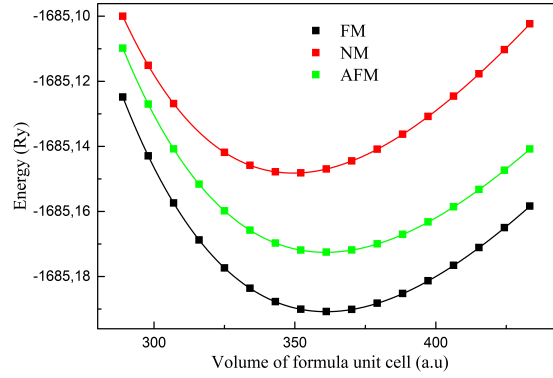
Figure 2. (Color online) Total energy as a function of the volume of the formula unit cell for $KBeO_3$ in its FM, NM and AFM phases.

parameter, bulk modulus B and its derivative B' are determined by fitting the curve of the total energy as a function of volume to the Birch-Murnaghan equation [20], given by the following expression:

$$E(V) = E_0 + \frac{9V_0 B_0}{16} \left\{ \left[\left(\frac{V_0}{V} \right)^{2/3} - 1 \right]^3 B_0 + \left[\left(\frac{V_0}{V} \right)^{2/3} - 1 \right]^2 \left[6 - 4 \left(\frac{V_0}{V} \right)^{2/3} \right] \right\} \quad (3.1)$$

Where E_0 is the equilibrium total energy, V_0 is the volume of the unit cell at zero pressure, B_0 and B'_0 are the bulk modulus and its pressure derivative, respectively. The $E(V)$ curves are illustrated in figure 2. From this figure, it can be seen that our compound is more stable energetically in its FM phase. We find the ground-state parameters (a_0, B_0 and B'_0), as shown in table 1. The obtained lattice parameter of FM phase agree very well with that of Persson [12].

Table 1. Calculated values of the equilibrium lattice parameter a_0 (in Å), bulk modulus B_0 (GPa) and its pressure derivative, and ground state energy E_0 (in Ry) for $KBeO_3$.

Phase	a_0	B	B'	$E_{\min}$
FM	3.7269 3.7716 [12]	97.3655	4.2529	-1685.148191
NM	3.7674	87.8309	4.1719	-3370.345067
AFM	3.7683	90.8969	4.2754	-1685.190774

The mechanical stability of a cubic system requires that Born's stability criteria should be met [21]: $C_{44} > 0$, $C_{11} - |C_{12}| > 0$, $C_{11} + 2C_{12} > 0$ and $C_{12} < B < C_{11}$, which reflects the stability of our material in this structure against elastic deformations. The calculations of elastic constants are performed, using the energy-strain approach implemented in the WIEN2k code [22], for the energetically favorable phase. The obtained values of the elastic constants C_{11}, C_{12} and C_{44} of the $KBeO_3$ compound, as well as those of [12], are listed in table 2.

According to Born's stability criteria, our compound is found to be mechanically stable in this phase while its instability is shown by Projector Augmented Wave (PAW) method, as implemented in the Vienna Ab Initio Simulation Package (VASP) software [23].This discrepancy is not due only to different methods used but can also be explained by the fact that, in the latter work, the used k-mesh of $6 \times 6 \times 6$ probably leads to inaccurate results and even to the prediction of a mechanically unstable phase.

Other quantities related to the elastic constants can be deduced, such as the shear modulus G, the Young's modulus E, the anisotropic parameter A, the ratio B/G and the Poisson's ratio ν. The obtained B/G ratio value of our material is higher than the critical value 1.75 which separates the ductile/brittle (brittle<1.75<ductile) behavior [24], as mentioned in table 2. Accordingly, our compound can be classified
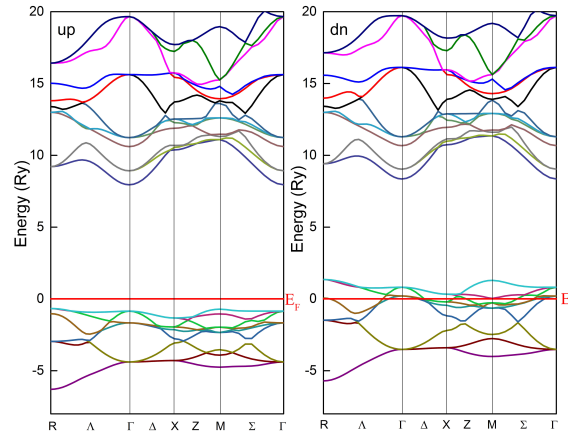
Figure 3. (Color online) Calculated spin-polarized band structures for KBeO$_3$ at its equilibrium lattice constant.

as a ductile material. As can be seen from table 2, the anisotropic parameter A is higher than 1. Thus, KBeO$_3$ exhibits an anisotropic character.

Table 2. Elastic constants C_{11}, C_{12}, C_{44}, bulk B, shear G, Young E moduli (in GPa), anisotropic parameter A, B/G ratio, and Poisson's ratio ν for KBeO$_3$

B	C_{11}	C_{12}	C_{44}	G	E	A	B/G	ν
97.180	124.0838	83.7281	45.7706	35.533	95.018	2.2683	2.73	0.337
112 [12]	90 [12]	124 [12]	41 [12]	−47 [12]		−5.8 [12]		0.75 [12]

To further confirm the stability of this compound, we calculated the formation energy, in order to examine the thermodynamic stability related to its synthesizability. The formation enthalpy can be computed by the following relation:

$$E_f(\text{KBeO}_3) = E_{\text{tot}}(\text{KBeO}_3) - E_{\text{Bulk}}(\text{K}) - E_{\text{Bulk}}(\text{Be}) - 3/2E(\text{O}_2) \tag{3.2}$$

where $E_{\text{Bulk}}(\text{K})$, $E_{\text{Bulk}}(\text{Be})$, and $E(\text{O}_2)$, correspond to the total energy for K, and Be, per atom, and for O$_2$ molecule, respectively. The obtained negative formation energy of −0.056 Ry indicates that KBeO$_3$ is thermodynamically stable. Therefore, it can be synthesized in the normal conditions.

3.2. Electronic properties

The importance of these properties makes it possible to analyze and understand the nature of the bonds between the different elements of a material. Band structures allow one to understand the phenomenon of half-metallic character in a compound. In this part, we performed electronic structure calculations for KBeO$_3$ where we use the equilibrium lattice constant corresponding to the FM phase. We used GGA, to calculate spin-polarized band structures, as shown in figure 3. It is clear that in the spin-dn band structure, the valence band (VB) and Fermi level overlap (i. e., intersect). This indicates that the compound shows a metallic behavior for this spin direction, whereas the spin-up band structure has a gap of 8.61 eV, which represents an insulating character. Therefore, KBeO$_3$ is half-metallic compound.

The total and partial densities of state for perovskite oxide KBeO$_3$ in its ferromagnetic phase are calculated at its structural equilibrium state using GGA, as illustrated in figure 4. From the total and partial densities, found by the FP-LAPW method, we can distinguish three important energy intervals. The first region is located at about [−7 eV, −0.63 eV] in both spin directions, the contribution of O-p orbital is dominant. In the second interval, there is a band gap of 8.61 eV in the spin-up around Fermi
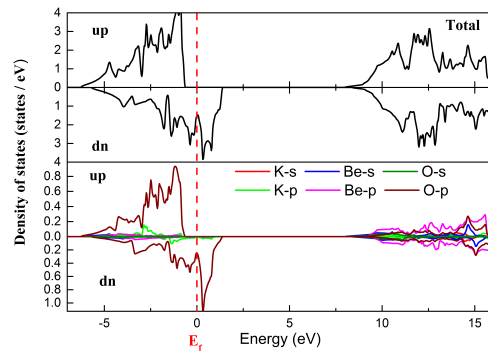
Figure 4. (Color online) Total and partial spin-dependent densities of states for $KBeO_3$ at its equilibrium lattice constant.

level. The conduction band, between [7.95 eV, 16 eV] is formed mainly by p orbitals of (K) ,(Be) and (O) atoms.

3.3. Magnetic properties

In this section, we begin to understand the magnetic character of $KBeO_3$ compound. As shown in table 3, the magnetic character comes mainly from O atoms. It can be seen that the main contribution to the magnetic character in the resulting DOS, obtained by the GGA method around the Fermi level, is due to the orbital p of O atoms. It is found that O has a larger magnetic moment. This result is confirmed by the results of the DOS (figure 4). The total magnetic moment of our studied compound has the integer value of $3\mu_B$. Such as our previously studied compounds $LiBeO_3$ and $KMgO_3$ [6, 7], the magnetic moment value of $3.0\mu_B$ can be clarified by the existance of 21 valence electrons in $KBeO_3$. The single valence electron of K and two electrons of Be are attracted by the Oxygen atoms. Therefore, the $KBeO_3$ valence electrons are distributed as follows: two electrons fill s-states of the O atoms and five electrons occupy their p-orbitals, giving rise to one unpaired electron for each O atom, leading to a total magnetic moment of $3.0\mu_B$. In contrast to transition and rare-earth-based perovskites such as $BaFeO_3$, $PrMnO_3$ and $BaNpO_3$ [8, 9, 11] with total magnetic moments of $6\mu_B$, $4\mu_B$, and $3\mu_B$, respectively, where the magnetism is originated from TM and RE elements, the contribution of the three O atoms of $KBeO_3$ ensures a comparable total magnetic moment.

To better highlight the origin of the magnetic moment of our considered compound, the spin density isosurfaces were plotted as shown in figure 5. It is clear from this figure that the spin magnetic moment is localized around O atoms which are shown to be ferromagnetically coupled, according to the yellow isosurfaces. Meanwhile, a part of spin magnetic moment around Be atom, as shown by blue drop shapes, indicates a small negative spin magnetic moment. On the other hand, there is no spin accumulated around K, signifying a negligible magnetic moment value of K.

Table 3. Calculated total, atom-resolved, and interstitial magnetic moments (in μ_B) in the unit cell for $KBeO_3$

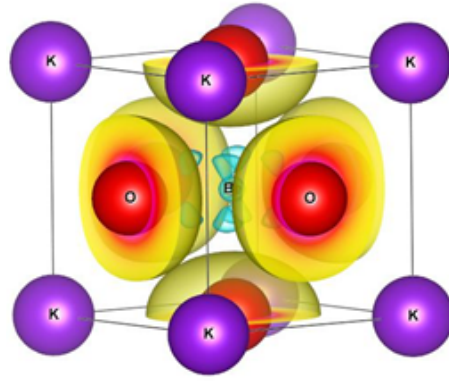| M_{tot}	M_K	M_{Be}	M_O	M_{int}
3.00068	0.01196	−0.01417	0.74613	0.76451

Figure 5. (Color online) Spin density of $KBeO_3$.

3.4. Pressure effect on the half-metallic character

Figure 6 shows the total, atomic, interstitial magnetic moments, valance band maximum, conduction band minimum in the spin-up direction, and spin-polarization as a function of the pressure for $KBeO_3$. It can be seen from this figure that the total magnetic moment maintains the value of $3\mu_B$, once the pressure reached 97 GPa, which corresponds to the lattice parameter value of 6.14 a.u., the total magnetic moment becomes zero 0 μ_B. At this pressure, a magnetic phase transition from FM to NM state may occur. This result agrees with the phase transition studied, as presented in figure 6. At 0 K, the datum of the pressure for the phase transition can be concluded from the ordinary condition of the same enthalpy $H = E + PV$. Regarding $KBeO_3$ compound, the variation of the enthalpy as a function of the pressure at 0 K is noted in figure 6, the crossing of enthalpy-pressure curves show that the value of transition pressure from FM to NM is about 97 GPa. The valence band maximum (VBM) and conduction band minimum (CBM) values in the spin-up direction are used to examine the effect of the pressure on the half-metallic stability for our compound studied (see figure 6).
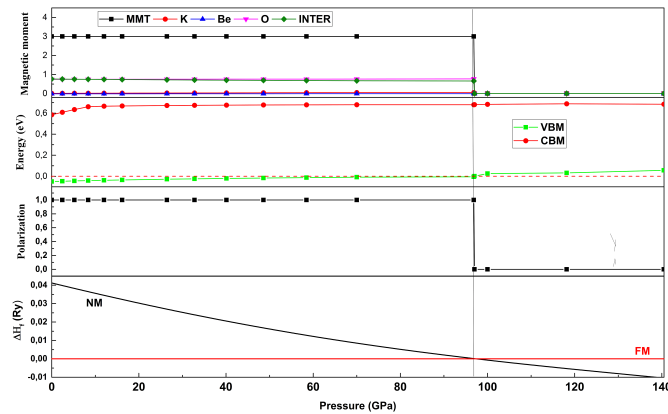

Figure 6. (Color online) Total, atomic, interstitial magnetic moments, CBM, VBM in the spin-up channel, spin polarization, and enthalpy as function of pressure for $KBeO_3$.

The spin polarization (P) at Fermi E_F level is related to spin-polarized DOS by the expression:

$$P(E_F) = \frac{|\rho_\uparrow(E_F) - \rho_\downarrow(E_F)|}{\rho_\uparrow(E_F) + \rho_\downarrow(E_F)}. \tag{3.3}$$

Where $\rho_\uparrow(E_F)$ and $\rho_\downarrow(E_F)$ are the majority and minority state densities at Fermi level E_F. As is clear from figure 6, the spin polarization at Fermi level is 100% up to the pressure of 97 GPa. As shown in this
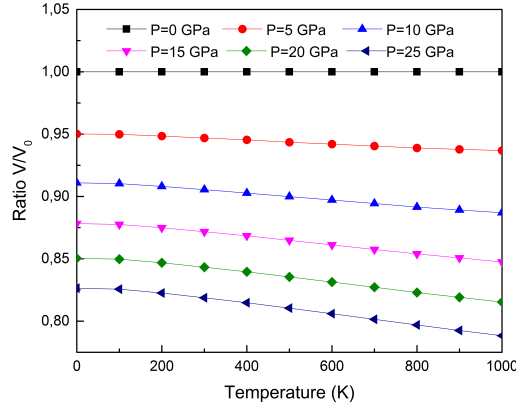
Figure 7. (Colour online) Pressure and temperature dependence of the relative volume V/V_0 for $KBeO_3$ (V_0 is the equilibrium volume).

figure, it can be seen that the half-metallicity character can be conserved up to 97 GPa. When the pressure value is bigger than 97 GPa, the half-metallicity is lost and the compound becomes a non-magnetic metal.

3.5. Thermodynamic properties

The thermodynamic properties of $KBeO_3$ are obtained by means of the quasi-harmonic Debye model [25, 26]. The non-equilibrium Gibbs function $G(V, P, T)$ is given by:

$$G^*(V, P, T) = E(V) + PV + A_{vib}[\theta(V), T] \tag{3.4}$$

Where $E(V)$ is the total energy of the unit cell for $KBeO_3$, PV is the constant hydrostatic pressure condition and the A_{vib} is the vibrational Helmholtz free energy, expressed by [25]:

$$A_{vib}(\theta_D, T) = nk_BT \left\{ 9\theta_D/8T + 3\ln[1 - e^{(-\theta_D/T)}] - D(\theta_D/T) \right\} \tag{3.5}$$

where n is the number of atoms per formula unit and the Debye integral $D(\theta_D/T)$, for an isotropic solid, is [25]:

$$\theta_D = \hbar/k_B(6\pi^2 nV^{1/2})^{1/3} f(\sigma)(B_s/M)^{1/2}. \tag{3.6}$$

Where, M is the molecular mass per unit cell. B_s is the adiabatic bulk modulus, which is approximately given by static compressibility [25]:

$$B_s = B(V) = V\frac{\partial^2 E(V)}{\partial V^2} \tag{3.7}$$

and $f(\sigma)$ is given by [25]:

$$f(\sigma) = \left\{ 3\left[2\left(\frac{21 + \sigma}{31 - 2\sigma} \right)^{3/2} + \left(\frac{11 + \sigma}{31 - \sigma} \right)^{3/2} \right] \right\}^{1/3} \tag{3.8}$$

where σ is Poisson ratio. The non-equilibrium Gibbs function $G^*(V, P, T)$, as a function of (V, P, T) can be minimized with respect to volume V as:

$$\left[\frac{\delta^2 G^*(P, V)}{\delta V^2} \right]_{P,V} = 0 \tag{3.9}$$

can be obtained by equation (3.9). The isothermal bulk modulus B_T is given by [26]:

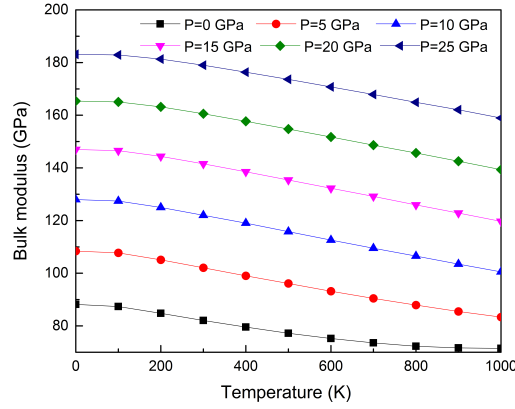$$B_T(P, T) = V\left[\frac{\delta^2 G^*(P, V, T)}{\delta V^2} \right]_{P,T} \tag{3.10}$$

Figure 8. (Colour online) Pressure and temperature dependence of the bulk modulus for $KBeO_3$.
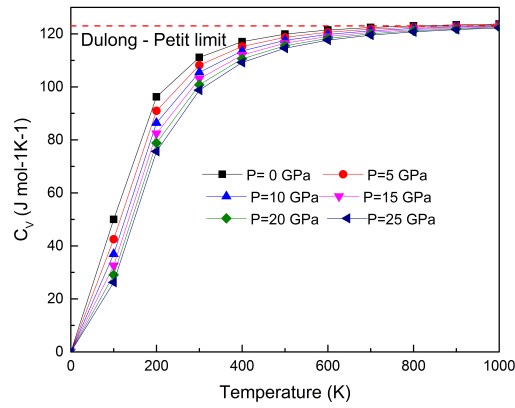

Figure 9. (Colour online) Pressure and temperature dependence of the heat capacity C_V for $KBeO_3$.

The thermodynamic quantities such as heat capacity at a constant volume C_V and entropy S are calculated by the relations[25, 26]:

$$C_V = 3nk_B \left[4D\left(\frac{\theta_D}{T}\right) - \frac{3\theta_D/T}{e^{\theta_D/T} - 1} \right] \tag{3.11}$$

$$S_V = nk_B \left[4D\left(\frac{\theta_D}{T}\right) - 3\ln(1 - e^{-\theta_D/T}) \right] \tag{3.12}$$

where the thermal expansion coefficient α is given by:

$$\alpha = \frac{\gamma C_V}{B_T T} \tag{3.13}$$

The thermal properties of $KBeO_3$, in its FM phase, are determined in the temperature range 0–1000 K for different pressures in the range 0–25 GPa. It is evident from figure 7 that the volume ratio V/V_0 decreases linearly with an increasing temperature at a given pressure and decreases with an increasing pressure at a given temperature. The bulk modulus relates to the change in the volume of an object, when subjected to pressure changes, and is used to describe hardness [27]. Figure 8 presents the variation of bulk modulus with temperature for particular pressures (0, 5, 10, 15, 20, 25 GPa). It is clearly seen that B is nearly stable between 0 to 100 K and decreases linearly with an increasing temperature. On the other hand, the compound loses its hardness with an increasing temperature. The bulk modulus, at zero pressure and $T=300$ K, is 82.07 GPa.

Figure 9 presents an examination for the relation between heat capacity at a constant volume (C_V) and temperature for 0, 5, 10, 15, 20, and 25 GPa pressures. At a lower temperature, C_V values grow rapidly
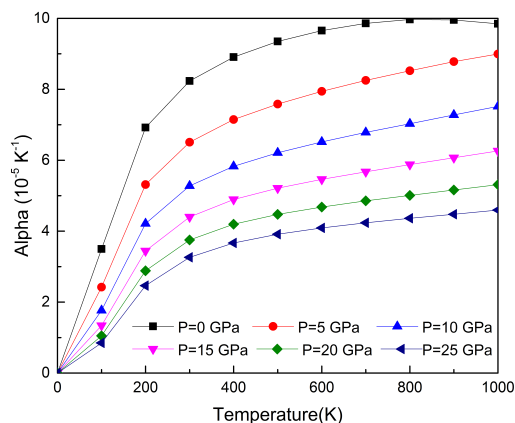
Figure 10. (Colour online) Pressure and temperature dependence of the thermal expansion for $KBeO_3$.
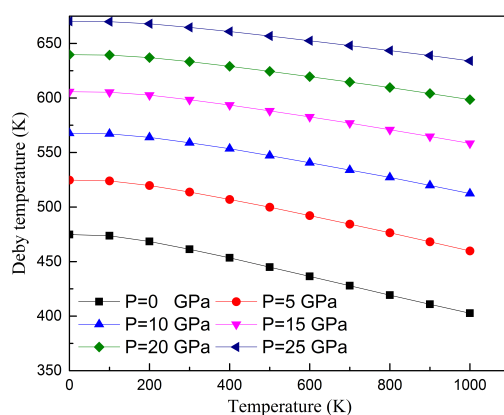

Figure 11. (Colour online) Pressure and temperature dependence of the Debye temperature for $KBeO_3$.

($T < 200$ K) and its evaluation is proportional to T^3 [27], then increases heavily at a higher temperature and approaches the Dulong-Petit limit [25]. Beyond about 800 K, C_V stays the same, its value is about 123 (J/mol K).

Another thermodynamic parameter for $KBeO_3$, the thermal expansion, is shown in figure 10, as a function of the temperature and pressure. It can be seen that the thermal expansion coefficient α increases pointedly with an increasing temperature up to 200 K. For higher temperature ($T > 200$ K), α progressively approaches a linear increase with temperature, which means that the temperature dependence of alpha is relatively low at high temperatures. At 300 K and zero pressure, the thermal expansion coefficient α value is 8.23×10^{-5} K^{-1} [28].

Figure 11 depicts the temperature and pressure effects on Debye temperature. From this figure, it can be seen that θ_D is nearly stable from 0 to 100 K and decreases with increasing the temperature. Moreover, it is evident that when the temperature is constant, the Debye temperature increases with the pressure applied. The Debye temperature of our compound at 0 GPa and 300 K temperature equals 461.25 K.

4. Conclusion

Using first-principles calculations, the half-metallicity has been predicted in $KBeO_3$, with the total magnetic moment of $3\mu_B$ per unit cell. The magnetism of this material mainly originates from the p orbital of O atoms. The results indicate that $KBeO_3$ is an anisotropic ductile material and keeps a perfect half-metallicity in the pressure range from 0 to 97 GPa. On the other hand, a transition occurs

from ferromagnetic to non-magnetic phase under this pressure value. Therefore, $KBeO_3$ is a promising material as a source material for spin injection and electrode materials for Giant Magneto-Resistance (GMR) devices. In addition, the thermodynamic properties are assessed using the quasi-harmonic Debye model.

References

1. Hemberger J., von Nidda H.A.K., Fritsch V., Deisenhofer J., Lobina S., Rudolf T., Lunkenheimer P., Lichtenberg F., Loidl A., Bruns D., Büchner B., Phys. Rev. Lett., 2003, **91**, 066403, doi:10.1103/PhysRevLett.91.066403.
2. Choi K.J., Biegalski M., Li Y., Sharan A., Schubert J., Uecker R., Reiche P., Chen Y., Pan X., Gopalan V., Chen L.-Q., Schlom D.G., Eom C.B., Science, 2004, **306**, 1005–1009, doi:10.1126/science.1103218.
3. Geday M., Glazer A., J. Phys. Condens. Matter, 2004, **16**, 3303, doi:10.1088/0953-8984/16/20/001.
4. Tagantsev A., Vaideeswaran K., Vakhrushev S., Filimonov A., Burkovsky R., Shaganov A., Andronikova D., Rudskoy A., Baron A., Uchiyama H., Chernyshov D., Bosak A., Ujma Z., Roleder K., Majchrowski A., Ko J.-H., Setter N., Nat. Commun., 2013, **4**, 2229, doi:10.1038/ncomms3229.
5. Sawada H., Hamada N., Terakura K., Physica B, 1997, **237**, 46–47, doi:10.1016/S0921-4526(97)00043-4.
6. Khelfaoui F., Amara K., Boutaleb H., Hamlat M., Boudia K., Abderrahmane Y.S., Marbouh N., Comput. Condens. Matter, 2019, **21**, e00399, doi:10.1016/j.cocom.2019.e00399.
7. Hamlat M., Boudia K., Amara K., Khelfaoui F., Marbouh N., Comput. Condens. Matter, 2020, **23**, e00456, doi:10.1016/j.cocom.2020.e00456.
8. Bouadjemi B., Bentata S., Abbad A., Benstaali W., Bouhafs B., Solid State Commun., 2013, **168**, 6–10, doi:10.1016/j.ssc.2013.06.008.
9. Rahman G., Sarwar S., Phys. Status Solidi B, 2016, **253**, 329–334, doi:10.1002/pssb.201552417.
10. Ali Z., Ahmad I., Khan B., Khan I., Chin. Phys. Lett., 2013, **30**, 047504, doi:10.1088/0256-307X/30/4/047504.
11. Khandy S.A., Gupta D.C., Mater. Chem. Phys., 2017, **198**, 380–385, doi:10.1016/j.matchemphys.2017.06.033.
12. Jain A., Ong S.P., Hautier G., Chen W., Richards W.D., Dacek S., Cholia S., Gunter D., Skinner D., Ceder G., Persson K.A., APL Materials, 2013, 1, 011002, doi:10.1063/1.4812323.
13. Blaha P., Schwarz K., Madsen G.K., Kvasnicka D., Luitz J., WIEN2k: An Augmented Plane Wave + Local Orbitals Program for Calculating Crystal Properties, Vienna University of Technology, Vienna, 2001.
14. Perdew J.P., Wang Y., Phys. Rev. B, 1992, **46**, 12947, doi:10.1103/PhysRevB.46.12947.
15. Perdew J.P., Ruzsinszky A., Csonka G.I., Constantin L.A., Sun J., Phys. Rev. Lett., 2009, **103**, 026403, doi:10.1103/PhysRevLett.103.026403.
16. Perdew J.P., Burke K., Ernzerhof M., Phys. Rev. Lett., 1996, **77**, 3865, doi:10.1103/PhysRevLett.77.3865.
17. Anisimov V.I., Solovyev I., Korotin M., Czyzyk M., Sawatzky G., Phys. Rev. B, 1993, **48**, 16929, doi:10.1103/PhysRevB.48.16929.
18. Blöchl P., Jepsen O., Andersen O.K., Phys. Rev. B, 1994, **49**, 16223, doi:10.1103/PhysRevB.49.16223.
19. Jamal M., Bilal M., Ahmad I., Jalali-Asadabadi S., J. Alloys Compd., 2018, **735**, 569–579, doi:10.1016/j.jallcom.2017.10.139.
20. Birch F., J. Geophys. Res. Solid Earth, 1978, **83**, 1257–1268, doi:10.1029/JB083iB03p01257.
21. Nye J.F., Physical Properties of Crystals: Their Representation by Tensors and Matrices, Oxford University Press, New York, 1985.
22. Jamal M., Asadabadi S.J., Ahmad I., Aliabad H.R., Comput. Mater. Sci., 2014, **95**, 592–599, doi:10.1016/j.commatsci.2014.08.027.
23. Sun G., Kurti J., Rajczy P., Kertesz M., Hafner J., Kresse G., J. Mol. Struct., 2003, 624, 37–45, doi:10.1016/S0166-1280(02)00733-9.
24. Pugh S., London, Edinburgh Dublin Philos. Mag. J. Sci., 1954, **45**, 823–843, doi:10.1080/14786440808520496.
25. Blanco M., Francisco E., Luana V., Comput. Phys. Commun., 2004, **158**, 57–72, doi:10.1016/j.comphy.2003.12.001.
26. Peng F., Fu H.Z., Cheng X.L., Physica B, 2007, **400**, 83–87, doi:10.1016/j.physb.2007.06.020.
27. Teter D.M., MRS Bull., 1998, **23**, 22–27, doi:10.1557/S0883769400031420.
28. Petit A.-T., Dulong, P.-L., Ann. Chim. Phys., 1819, **10**, 395–413.

Індукований високим тиском магнітний фазовий перехід у напівметалічному перовскіті KBeO$_3$

М. Хамлат[1], К. Амара[1], К. Будіа[2], Ф. Хелфаї[1] Г. Буталеб[1]

[1] Фізико-хімічна лабораторія, Університет ім. D$^\text{г}$ Тахара Мулая м. Саїда, 20000 Саїда, Алжир

[2] Фізико-хімічна лабораторія новітніх матералів, Університет Джиллалі Ліабеса, 22000 Сіді-Бель-Аббес, Алжир

У статті досліджуються структурні, механічні, магнітно-електронні і термодинамічні властивості перовскіту KBeO$_3$. Обчислення здійснено повно-потенціальним методом приєднаних плоских хвиль, імплементованим в WIEN2k коді, який базується на теорії функціоналу густини з використанням узагальненого градієнтного наближення. Обчислена енергія формування і пружні константи вказують на здатність синтезуватися і механічну стійкість KBeO$_3$. Більше того, наші результати показали, що KBeO$_3$ є напівметалічним матеріалом з напівметалічною забороненою зоною 0.67 eV та сумарним магнітним моментом 3μ_B на елементарну комірку. Окрім цього, KBeO$_3$ утримує напівметалічний характер під дією тиску аж до 97 GPa, що відповідає передбачуваному переходу магнітної фази з феромагнітного в немагнітний стан. Квазігармонічну модель Дебая використано для аналізу об'ємного коефіцієнта V/V_0, об'ємного модуля, питомої теплоємності, температурного розширення та температури Дебая.

Ключові слова: перовскіт, напівметалічний характер, механічна стійкість, перехід магнітної фази, термодинамічні властивості